

## Photosynthesis-driven methane production in oxic lake water as an important contributor to methane emission

Marco Günthel<sup>1\*</sup>, Isabell Klawonn<sup>2</sup>, Jason Woodhouse<sup>2</sup>, Mina Bižić<sup>2</sup>, Danny Ionescu<sup>2</sup>, Lars Ganzert<sup>1b</sup>,<sup>2</sup> Steffen Kümmel<sup>3</sup>, Ivonne Nijenhuis<sup>3</sup>, Luca Zoccarato<sup>2</sup>, Hans-Peter Grossart<sup>1b,2,4\*</sup>, Kam W. Tang<sup>1\*</sup>

<sup>1</sup>Department of Biosciences, Swansea University, Swansea, United Kingdom

<sup>2</sup>Department of Experimental Limnology, Leibniz Institute of Freshwater Ecology and Inland Fisheries, Stechlin, Germany

<sup>3</sup>Department for Isotope Biogeochemistry, Helmholtz Centre for Environmental Research-UFZ, Leipzig, Germany

<sup>4</sup>Institute of Biochemistry and Biology, Potsdam University, Potsdam, Germany

### Abstract

Recent discovery of methane (CH<sub>4</sub>) production in oxic waters challenges the conventional understanding of strict anoxic requirement for biological CH<sub>4</sub> production. High-resolution field measurements in Lake Stechlin, as well as incubation experiments, suggested that oxic-water CH<sub>4</sub> production occurred throughout much of the water column and was associated with phytoplankton especially diatoms, cyanobacteria, green algae, and cryptophytes. In situ concentrations and δ<sup>13</sup>C values of CH<sub>4</sub> in oxic water were negatively correlated with soluble reactive phosphorus concentrations. Using <sup>13</sup>C-labeling techniques, we showed that bicarbonate was converted to CH<sub>4</sub>, and the production exceeded oxidation at day, but was comparable at night. These experimental data, along with complementary field observations, indicate a clear link between photosynthesis and the CH<sub>4</sub> production-consumption balance in phosphorus-limited epilimnic waters. Comparison between surface CH<sub>4</sub> emission data and experimental CH<sub>4</sub> production rates suggested that the oxic CH<sub>4</sub> source significantly contributed to surface emission in Lake Stechlin. These findings call for re-examination of the aquatic CH<sub>4</sub> cycle and climate predictions.

The widely reported “methane paradox,” that is, oversaturation of dissolved methane (CH<sub>4</sub>) in oxic sea and lake waters (Tang et al. 2016), contradicts the conventional understanding that biological CH<sub>4</sub> production occurs exclusively under anoxic conditions (Thauer 1998; Ferry and Kestead 2007).

Research in recent years has shown that active CH<sub>4</sub> production occurs in oxic sea (Karl et al. 2008; Damm et al. 2010) and lake waters (Grossart et al. 2011; Bogard et al. 2014; Tang et al. 2014). Globally, freshwaters account for about 122 ± 60 Tg yr<sup>-1</sup> or about 20% of CH<sub>4</sub> emission to air (Saunois et al. 2016) and their contribution is expected to increase in future climate change scenarios (Dean et al. 2018). It is therefore necessary to understand the environmental dynamics of this oxic-water CH<sub>4</sub> source and its potential contribution to CH<sub>4</sub> emission to the atmosphere.

We investigated oxic-water CH<sub>4</sub> production in Lake Stechlin (Northeast Germany), an oligo-mesotrophic glacial lake in the temperate region that has been intensively monitored for decades (Casper 1985). Biological productivity in Lake Stechlin is phosphorus-limited (Casper 1985). Accordingly, the ratio of total nitrogen to total phosphorus in the epilimnion was (mean ± SD) 36 ± 9 during the study period in 2016 (March–July; *n* = 15) (Supporting Information Fig. S1), much higher than what is considered to indicate phosphorus limitation (i.e., a ratio of > 15 to > 22; Guildford et al. 2000; Abell et al. 2010). Recurring seasonal development of CH<sub>4</sub> oversaturation in the oxic midwater column has been observed in this lake, and previous studies have shown in situ oxic CH<sub>4</sub> production irrespective of CH<sub>4</sub> input from the sediment or lateral transport from the shore (Grossart et al. 2011; Tang et al. 2014). Despite skepticism (Fernandez et al.

\*Correspondence: hgrossart@igb-berlin.de (H.-P.G.); marcoguenthel@gmail.com (M.G.); k.w.tang@swansea.ac.uk (K.W.T.); [Leibniz-Institut für Gewässerökologie und Binnenfischerei (IGB) im Forschungsverbund Berlin e.V.]

This is an open access article under the terms of the Creative Commons Attribution License, which permits use, distribution and reproduction in any medium, provided the original work is properly cited.

Additional Supporting Information may be found in the online version of this article.

Current affiliation of Lars Ganzert: Geomicrobiology Department, Helmholtz-Centre Potsdam GFZ, 14473 Potsdam, Germany  
**Author Contribution Statement:** M.G., H.-P.G., and K.W.T. conceived the study. M.G., I.K., J.W., D.I., L.G., L.Z., and M.B. collected the field data. M.G., I.K., J.W., M.B., S.K., and I.N. collected the lab data. M.G. analyzed the data with input from coauthors. M.G. and K.W.T. wrote the manuscript with input from coauthors.

Correction added on 29 October 2020, after first online publication: [Leibniz-Institut für Gewässerökologie und Binnenfischerei (IGB) im Forschungsverbund Berlin e.V.] was added for [Marco Günthel]

2016; Peeters et al. 2019), mounting evidence for oxic-lake water CH<sub>4</sub> production suggests that this is a widespread phenomenon in lakes (Grossart et al. 2011; Bogard et al. 2014; Tang et al. 2014; Donis et al. 2017; DelSontro et al. 2018; Günthel et al. 2019; Khatun et al. 2019). Currently, there are two proposed pathways for oxic-lake water CH<sub>4</sub> production: (1) Methane as a by-product of methylphosphonate (MPN) decomposition, which is an alternative way of phosphorus acquisition when inorganic phosphorus is limited (Carini et al. 2014; Yao et al. 2016; Wang et al. 2017); and (2) a pathway independent of MPN demethylation which is thought to be based on a Coenzyme-M homologue (Tang et al. 2016). Several studies have demonstrated the involvement of photoautotrophs in CH<sub>4</sub> formation in oxic water, both in the field (Grossart et al. 2011; Bogard et al. 2014; Hartmann et al. 2020) and in the laboratory (Lenhart et al. 2016; Klitzsch et al. 2019; Bizic et al. 2020; Hartmann et al. 2020). The association of oxic CH<sub>4</sub> production to MPN degradation and autotrophic organisms suggests that phosphorus and light might be important factors driving oxic CH<sub>4</sub> production.

We conducted a comprehensive study of the CH<sub>4</sub> dynamics in the oxic water of Lake Stechlin in order to address these questions: Which environmental factors promote oxic CH<sub>4</sub> production? How is oxic CH<sub>4</sub> production connected to phytoplankton? What is the contribution of this production to water-to-air CH<sub>4</sub> flux? To investigate the environmental parameters that promote oxic CH<sub>4</sub> production, we statistically analyzed the temporal and spatial CH<sub>4</sub> distributions and its isotopic signatures and different biotic and abiotic factors in the lake on seasonal, weekly, and diurnal time scales. Field observations were complemented by incubation experiments manipulating light and phosphorus availability. To test for the involvement of phytoplankton, we further analyzed *in situ* CH<sub>4</sub> concentration together with chlorophyll and taxon-specific pigment fluorescence data. Additionally, we conducted incubation experiments to measure depth-specific and size-specific CH<sub>4</sub> production rates, as well as incubation experiments with pure diatom culture. Using <sup>13</sup>C-labelling techniques, we showed that bicarbonate was converted to CH<sub>4</sub> in lake water, thereby establishing a direct link between photoautotrophic carbon fixation and oxic CH<sub>4</sub> production. The <sup>13</sup>C-label experiment was designed to quantify CH<sub>4</sub> production and consumption simultaneously throughout the diurnal cycle providing information about the effect of light on the CH<sub>4</sub> production-consumption balance. Last, the contribution of oxic CH<sub>4</sub> production to the water-to-air CH<sub>4</sub> flux was examined by comparing oxic production rates from incubation experiments with CH<sub>4</sub> emission rates to the atmosphere.

## Materials and methods

### Field measurements

#### Lake characteristics and sampling sites

Lake Stechlin is a dimictic meso-to-oligotrophic lake in Northeastern Germany. The lake has three basins with a combined surface area of 4.25 km<sup>2</sup> (volume ca. 0.09 km<sup>3</sup>), a

shoreline of 16.1 km and a catchment area of about 12.4 km<sup>2</sup> (26 km<sup>2</sup> subsurface catchment area). With 69.5 m maximum depth and 22.8 m mean depth, it is one of Germany's deepest lakes. More details can be accessed online via the monitoring station of the Leibniz-Institute of Freshwater Ecology and Inland Fisheries (<https://www.igb-berlin.de/en/monitoring/stechlin>) or the World Lake Database hosted by the International Lake Environment Committee (<http://wldb.ilec.or.jp/Details/Lake/EUR-31>).

Two locations in Lake Stechlin were sampled: (1) the northeast basin (69.5 m deep site; 53°09'20.2"N 13°01'51.5"E) and (2) the south basin (20.5 m deep site; 53°08'36.6"N 13°01'43.0"E). Data obtained for the northeast basin include environmental parameters (YSI probe data, partial BBE probe data, nutrients), CH<sub>4</sub> concentration profiles (0–20 m depth; March–July 2016), carbon isotope signatures of water column CH<sub>4</sub>, and CH<sub>4</sub> surface emission rates. Data for the south basin sampling site include environmental parameters (YSI probe data, complete BBE probe data) and CH<sub>4</sub> concentration profiles (0–20 m depth; April–July 2016). Weather data were provided by the German Environment Agency (Neuglobsow weather station located directly next to the lake). Water samples collected for incubation experiments were collected in the south basin.

#### Environmental parameters

A YSI sonde Model 6600V2 was used to record temperature, dissolved oxygen, photosynthetically active radiation (PAR), and chlorophyll fluorescence. Concentrations of taxon-specific phytoplankton pigments were measured by a BBE Moldaenke Fluoroprobe. Parameter profiles were taken weekly during March–July 2016 at the deepest point (at 0, 2, 4, 6, 7, 8, 9, 10, 12, 14, 16, 18, and 20 m depth; YSI) and continuously every hour in the southern basin (0.5–20 m depth in 0.5 m intervals; YSI and BBE).

Nutrient concentrations were measured photometrically using a Foss Analytical FIAstar 5000 Analyzer with DDW detector and common standards: total phosphate (AN 5241, ISO 15681-1), soluble reactive phosphate (AN 5240, ISO 15681-1), total nitrogen (AN 5202D, DIN EN ISO 13395, ISO 11905), and NH<sub>4</sub>-nitrogen (AN 5220, ISO 11732). Nutrient data were obtained weekly (May–July 2016) at 4, 7, 8, 10, and 12 m depth (deepest point).

#### Methane concentrations

Water was transferred from a Limnos Water Sampler to 50 mL serum bottles (clear borosilicate glass, ≥ 88% transmission of PAR spectrum), which were flushed three times then crimp-closed (PTFE-butyl septa, aluminum caps) without gas bubbles. Dissolved CH<sub>4</sub> was extracted using head space (Helium) displacement method and measured by a Shimadzu 14A GC/FID (35°C Permabond FFAP column on N<sub>2</sub>, split-less injection, and detection at 140°C). Headspace CH<sub>4</sub> was converted to dissolved CH<sub>4</sub> concentrations based on Henry's Law and standard conditions. Seasonal CH<sub>4</sub> data were obtained in a 1-week interval; diurnal CH<sub>4</sub> data were collected

in 6-h intervals (only the last data point delayed by 1 h) from 8<sup>th</sup> July 2016 at 14:00 h local time until 11<sup>th</sup> July 2016 at 15:00 h (14:00 +  $n \times 6$  h; 13 profiles). The standard deviations of measurements (averaged over depths) were  $\pm 0.004$  (north-east basin, triplicates) and  $\pm 0.009$  (south basin, duplicates) for the seasonal data, and  $\pm 0.016 \mu\text{mol L}^{-1}$  (south basin, duplicates) for the diurnal data.

### Methane emission

Emitted  $\text{CH}_4$  was captured by a 15-liter floating chamber that was submerged at the perimeter by 3 cm and had a tube (butyl septum) at the center for gas sampling. Over 1–2 h, nine gas samples of each 20 mL were withdrawn by syringe, transferred into 50 mL serum bottles (prefilled with NaCl-saturated distilled water; PTFE septa enclosed), and the  $\text{CH}_4$  concentrations were measured with GC/FID as described earlier. The  $\text{CH}_4$  surface flux was then derived from linear regression over time.

### Carbon isotope signature of water column methane

Anoxic sediment methanogenesis produces  $\text{CH}_4$  with  $\delta^{13}\text{C}$  values typically less than  $-55\text{‰}$  (Whiticar 1999; Conrad et al. 2007). Methane oxidation at the sediment-water interface and within the water column preferentially enriches the  $^{13}\text{C}$  content in the  $\text{CH}_4$  pool, leading to  $\delta^{13}\text{C}$  values greater than  $-55\text{‰}$  in the water column (i.e., Whiticar 1999; Tang et al. 2014). Accordingly, changing water column  $\delta^{13}\text{C}$  signatures to more negative values are commonly attributed to  $\text{CH}_4$  production whereas changes to more positive values are attributed to  $\text{CH}_4$  oxidation (Donis et al. 2017; DelSontro et al. 2018). The discovery of oxic  $\text{CH}_4$  production, however, requires re-evaluation of this assumption. We used the water column  $^{13}\text{C}$  signatures of  $\text{CH}_4$  to statistically analyze its relation to environmental parameters.

To analyze the carbon isotope signature of water column  $\text{CH}_4$ , 5 mL gas samples extracted from lake water at different depths were stored in 12 mL Exetainer (prefilled with NaCl-saturated distilled water) and analyzed with a GC/C-IRMS unit composed of Agilent 7890A GC, GC IsoLink, a ConFlo IV interface to a MAT 253 IRMS (Thermo Fisher) and a programmed temperature vaporizer (MMI G3510A/G3511A, Agilent Technologies) with glass liner (1 cm CarboSieve SIII 60/80 packing). Compressed sample injection was done at  $-90^\circ\text{C}$  (for 5.20 min, ramp  $600^\circ\text{C min}^{-1}$  until  $225^\circ\text{C}$ ). A Mol-Sieve 5A column ( $50 \text{ m} \times 0.32 \text{ mm} \times 30 \mu\text{m}$ ) running on  $2 \text{ mL min}^{-1}$  He ( $35^\circ\text{C}$  for 10 min, ramp  $20^\circ\text{C min}^{-1}$  until  $250^\circ\text{C}$ , final hold for 5 min) enabled separation. Carbon isotope signatures (of  $\text{CH}_4$ ) are expressed in conventional  $\delta^{13}\text{C}$  notation (‰) relative to Vienna-PeeDee Belemnite and were correlated to field parameter together with  $\text{CH}_4$  concentration.

### Linear modeling

R-software (R v3.3.1, RStudio v1.0.153) (RStudio Team, 2016) was used to test for linear relationships between parameters using general linear models, which were set up for  $\gamma$ -distribution and log-link, without interaction term unless

stated otherwise. Regression results shown in scatter plots are based on LM models. Supporting Information Table S1 summarizes the correlations.

## Experimental setups

### Size fractionation experiment

A substantial part of the phytoplankton community was larger than freshwater methanogenic Archaea (commonly  $< 20 \mu\text{m}$ ; Lyu and Liu 2019), and included cyanobacteria, diatoms, and green algae (Supporting Information Fig. S2). In this experiment, we examined which size fraction was responsible for  $\text{CH}_4$  production in the oxic water, considering the fractions  $< 20 \mu\text{m}$ ,  $> 20 \mu\text{m}$ , and nonfractionated.

One liter of an integrated lake water sample (4–8 m depth), taken on 3<sup>rd</sup> July 2018, was filtered through a  $20 \mu\text{m}$  net creating the  $< 20 \mu\text{m}$  size fractions. Afterward, the filter was inverted and  $> 20 \mu\text{m}$  particles were resuspended in 1 L of sterile-filtered ( $0.2 \mu\text{m}$ ) lake water, creating the  $> 20 \mu\text{m}$  size fraction. Unfiltered lake water was used as control. Water samples were added to 50 mL serum bottles (clear borosilicate glass,  $\geq 88\%$  transmission of PAR spectrum), air-saturated by bubbling atmospheric air for 10 min through a  $0.2 \mu\text{m}$  filter and crimp-closed. Two bottles per size fraction were incubated for 24 h under natural day light exposure in the laboratory. Methane concentration was measured by a GC/FID unit and net  $\text{CH}_4$  production was calculated as changing  $\text{CH}_4$  concentration divided by incubation time.

### Depth-specific methane production

Lake water from different depths was sampled in duplicates on 13<sup>th</sup> June 2016 and incubated in serum bottles (clear borosilicate glass,  $\geq 88\%$  transmission of PAR spectrum) in the laboratory exposed to natural daylight (on a shaker; room temperature). The  $\text{CH}_4$  concentration was measured by GC/FID on day 0, 14, and 21. The average  $\text{CH}_4$  production was calculated as changing  $\text{CH}_4$  concentration divided by incubation time for two periods: day 0–14 (using  $\text{CH}_4$  concentrations recorded on day 0 and 14) and day 0–21 (using  $\text{CH}_4$  concentrations recorded on day 0 and 21).

### $^{13}\text{C}$ labeling experiment

To investigate the role of phytoplankton in oxic  $\text{CH}_4$  production, lake water samples were spiked with dissolved inorganic carbon (DIC) as  $^{13}\text{C}$ -labeled bicarbonate. The conversion of DIC to  $\text{CH}_4$  was then measured as the incorporation of the  $^{13}\text{C}$  label into the  $\text{CH}_4$  product pool (IRMS analysis). Additionally, to quantify the  $\text{CH}_4$  production-consumption balance in oxic water at different time of day,  $\text{CH}_4$  oxidation was measured simultaneously by measuring the conversion of  $^{13}\text{C}$ -labeled  $\text{CH}_4$  to DIC.

Lake water (from 7 m depth) was collected on 1<sup>st</sup> September 2016, transferred to 12-mL Exetainer (clear soda lime glass,  $\geq 91\%$  transmission of PAR spectrum). To measure  $\text{CH}_4$  production, three treatment groups were set up: (1) no  $\text{DI}^{13}\text{C}$  addition, (2) addition of  $\text{DI}^{13}\text{C}$ , and (3) addition of  $\text{DI}^{13}\text{C}$  and  $1.4 \text{ mmol L}^{-1}$  methyl fluoride (inhibitor of  $\text{CH}_4$  oxidation; Chan and Parkin 2000) for control.  $\text{DI}^{13}\text{C}$  was added in the

form of  $^{13}\text{C}$ -labeled  $\text{NaHCO}_3$  to a final labeling percentage of 21%. To measure  $\text{CH}_4$  oxidation, three additional treatment groups were set up: (4) no  $^{13}\text{CH}_4$  addition, (5) addition of  $^{13}\text{CH}_4$ , and (6) addition of  $^{13}\text{CH}_4$  and  $1.4 \text{ mmol L}^{-1}$  methyl fluoride for control. The  $^{13}\text{CH}_4$  was added to a final labeling percentage of 92.5%. Each treatment group included exetainers for the following time points ( $t_n$ ; triplicate measurements): 0.3, 6.5, 15.5, 20.3, and 25.5 h (only first and last time points for the controls). All exetainers were placed in the lake at the original sampling depth and exposed to the ambient conditions; incubation started simultaneously at 16:00 h on 1<sup>st</sup> September 2016 (local time). After incubation, the corresponding water samples ( $t_n$ ) were retrieved from the lake and microbial activity was stopped by adding  $100 \mu\text{L}$   $\text{ZnCl}_2$  (saturated solution) per exetainer. For each time point, the  $^{13}\text{C}$  content in the product pool ( $\text{CH}_4$  for production; DIC for oxidation) was measured: Concentrations and  $^{13}\text{C}$  signatures of  $\text{CH}_4$  and DIC were measured by UC Davis (<https://stableisotopefacility.ucdavis.edu/index.html>). By comparing the  $^{13}\text{C}$  content in the product pool between time  $t_n$  and start time  $t_0$ , the  $^{13}\text{C}$  excess was calculated, which indicates average production/oxidation rates throughout the incubation periods (relative to how much substrate was labeled with  $^{13}\text{C}$ ).

The dimension of  $\text{CH}_4$  oxidation and  $\text{CH}_4$  production ( $\text{pmol L}^{-1} \text{ h}^{-1}$ ) were calculated as follows:

$$\text{CH}_4 \text{ Oxidation} = \frac{C_{\text{DIC, total}} * ^{13}\text{C atom\% excess}}{t * \text{CH}_4 \text{ substrate label}} \quad (1)$$

$$\text{CH}_4 \text{ Production} = \frac{C_{\text{CH}_4, \text{ total}} * ^{13}\text{C atom\% excess}}{t * \text{DIC substrate label}} + |\text{CH}_4 \text{ Oxidation}| \quad (2)$$

Here,  $C_{\text{DIC/CH}_4, \text{ total}}$  refers to overall concentration of DIC or  $\text{CH}_4$ ;  $^{13}\text{C atom\% excess}$  (%) is the enrichment of  $^{13}\text{C}$  in the sample computed via Eq. 3.  $t$  is the incubation time ( $t_n - t_0$ ),  $t_n$  is sampling time point, and  $t_0$  is starting time point. The *substrate label* is the of labeled substrates to the overall DIC or  $\text{CH}_4$  (0.21 or 0.925).

$$^{13}\text{C atom\% excess} = ^{13}\text{C atom\%}(t_n) - ^{13}\text{C atom\%}(t_0) \quad (3)$$

$^{13}\text{C atom\%}$  is the percentage of  $^{13}\text{C}$  in the sample, calculated from Eq. 4:

$$^{13}\text{C atom\%} = \frac{100 * \text{nat. } ^{13}\text{C ratio} * \frac{\delta^{13}\text{C}_{\text{VPDB}}}{100 + 1}}{1 * ^{13}\text{C ratio} * \frac{\delta^{13}\text{C}_{\text{VPDB}}}{100 + 1}} \quad (4)$$

where  $\delta^{13}\text{C}_{\text{VPDB}}$  is the relative deviation of sample  $^{13}\text{C}$  from Vienna-PeeDee Belemnite  $^{13}\text{C}$  (‰) and nat.  $^{13}\text{C}$  ratio refers to the natural abundance of  $^{13}\text{C}$  isotopes.

### Phosphorus addition experiment

In this experiment, we tested whether the addition of inorganic phosphorus to the lake water would affect the  $\text{CH}_4$  production-

consumption balance. An integrated lake water sample (4–8 m depth) was taken on 29<sup>th</sup> June 2018, filtered through a  $100 \mu\text{m}$  net, mixed carefully by shaking, then added to serum bottles (clear borosilicate glass,  $\geq 88\%$  transmission of PAR spectrum) without disturbing the ambient gas conditions and crimp-closed (Teflon coated septa). The water sample was either untreated or enriched with  $2.1 \text{ nmol}$  (per  $50 \text{ mL}$ )  $\text{K}_2\text{HPO}_4$  daily, and was incubated in the laboratory under natural day light exposure or in the dark. Microbial activity was stopped after incubation by adding  $\text{ZnCl}_2$  to a final concentration of  $0.5\%$ .  $\delta^{13}\text{C}$  of  $\text{CH}_4$  (GC/IRMS; 2–5 measurements), soluble reactive phosphorus (SRP; Foss Analytical FIStar 5000 Analyzer, one bottle sacrificed per time point), and oxygen saturation (PreSense sensor, one bottle sacrificed per time point) were measured at the start, and after 5 and 10 d of incubation.

### Pure culture experiment

We measured the  $\text{CH}_4$  production by two diatom cultures: *Navicula* sp. (isolated from Lake Stechlin) and *Leptocylindrus danicus* (marine), using a membrane inlet mass spectrometer (MIMS) and following the procedure of Bizic et al. (2020). The MIMS device (Bay Instruments, MD, U.S.A.) consisted of a crossbeam ion source mass spectrometer (Pfeiffer Vacuum, Germany), HiCube 80 Eco turbo pumping station (Pfeiffer Vacuum, Germany), QMG 220 M1, PrismaPlus<sup>®</sup>, C-SEM, 1–100 amu, and an experimental chamber. The experimental chamber (3.5 mL) contained an inner chamber for the culture and an outer chamber connected to a water bath to stabilize the temperature. The cultures were continuously mixed by a magnetic stirrer, kept at constant temperature, and incubated for 3 or 4 d under the following light regime: 19:30–09:00 h no light, gradually increasing to 60, 120, 180, and  $400 \mu\text{mol photon m}^{-2} \text{ s}^{-1}$  (1.5 h hold) then gradually decreasing in reverse order. A peristaltic pump (Minipuls3, Gibson) circulated the diatom cultures (constant temperature) continuously through a capillary linked to Viton pump tubing (Kana et al. 2006) kept in a water bath to stabilize the temperature and back to the culture (semi-closed system: no liquid loss, only gas loss). Throughout the circulation, the culture passed a microbore silicone membrane (8 mm, Silastic<sup>®</sup>, DuPont) permeable only to gases. The surrounding vacuum removed dissolved gases from the culture medium and fed it to the mass spectrometer where corresponding  $m/z$  ratios were recorded. The MIMS setup was calibrated to measure mass/charge ratio ( $m/z$ ) in MilliQ water and growth media at different temperatures. Further calibration was realized by making measurements on air-saturated MilliQ water at different salinities.

To start, 3.5 mL culture were transferred to the experimental chamber and the  $m/z$  ratios representative of  $\text{CH}_4$  (15) and oxygen (32) were recorded in a 9 s interval relative to the  $m/z$  ratio of argon ( $m/z = 40$ ). Concentrations of  $\text{CH}_4$ , oxygen, and argon were calculated using published solubilities (Powell 1972). Production rates of  $\text{CH}_4$  were calculated by first smoothing the raw data (sgolay function of the R package signal; 20 min interval; signal developers) (Signal Developers 2013) and then applying the 1<sup>st</sup> derivative. The degassing rate resulting from gas

consumption by the MIMS unit was determined experimentally and added to the absolute values of the 1<sup>st</sup> derivative. Final CH<sub>4</sub> production rates are presented relative to dry weight of the diatom biomass. To determine the dry weight, 3.5 mL diatom culture aliquot was filtered through a GF/F filter (combusted and preweighed; Millipore); the filter cake was subsequently dried (105°C) for 48 h and weighed at room temperature.

## Results

### Environmental setting

#### Seasonal scale

Seasonal CH<sub>4</sub> and environmental data for the south basin are presented in Fig. 1a–d and Supporting Information Fig. S3.

Preliminary measurements prior to the seasonal study showed low CH<sub>4</sub> concentrations in the upper 20 m in the northeast basin, on average 0.02 and 0.03  $\mu\text{mol L}^{-1}$  in February and March, respectively. As the lake began to stratify, upper water CH<sub>4</sub> concentration increased along with water temperature, reaching up to 1.4  $\mu\text{mol L}^{-1}$  in late June at the thermocline depth (Fig. 1a). Strong CH<sub>4</sub> accumulations were consistently found in waters with oversaturated dissolved oxygen (up to 167%; 17  $\text{mg L}^{-1}$ ). Methane concentrations at 0–20 m depth were positively correlated with temperature ( $p < 0.001$ ), PAR ( $p < 0.001$ ), and oxygen saturation (up to 167% saturation) ( $p < 0.001$ ). The concurrent total phosphorus was  $< 20 \mu\text{g L}^{-1}$ , SRP  $< 8 \mu\text{g L}^{-1}$ , total nitrogen  $< 1 \text{ mg L}^{-1}$ , and ammonium  $< 0.05 \text{ mg L}^{-1}$ . Further positive correlations were found between CH<sub>4</sub>

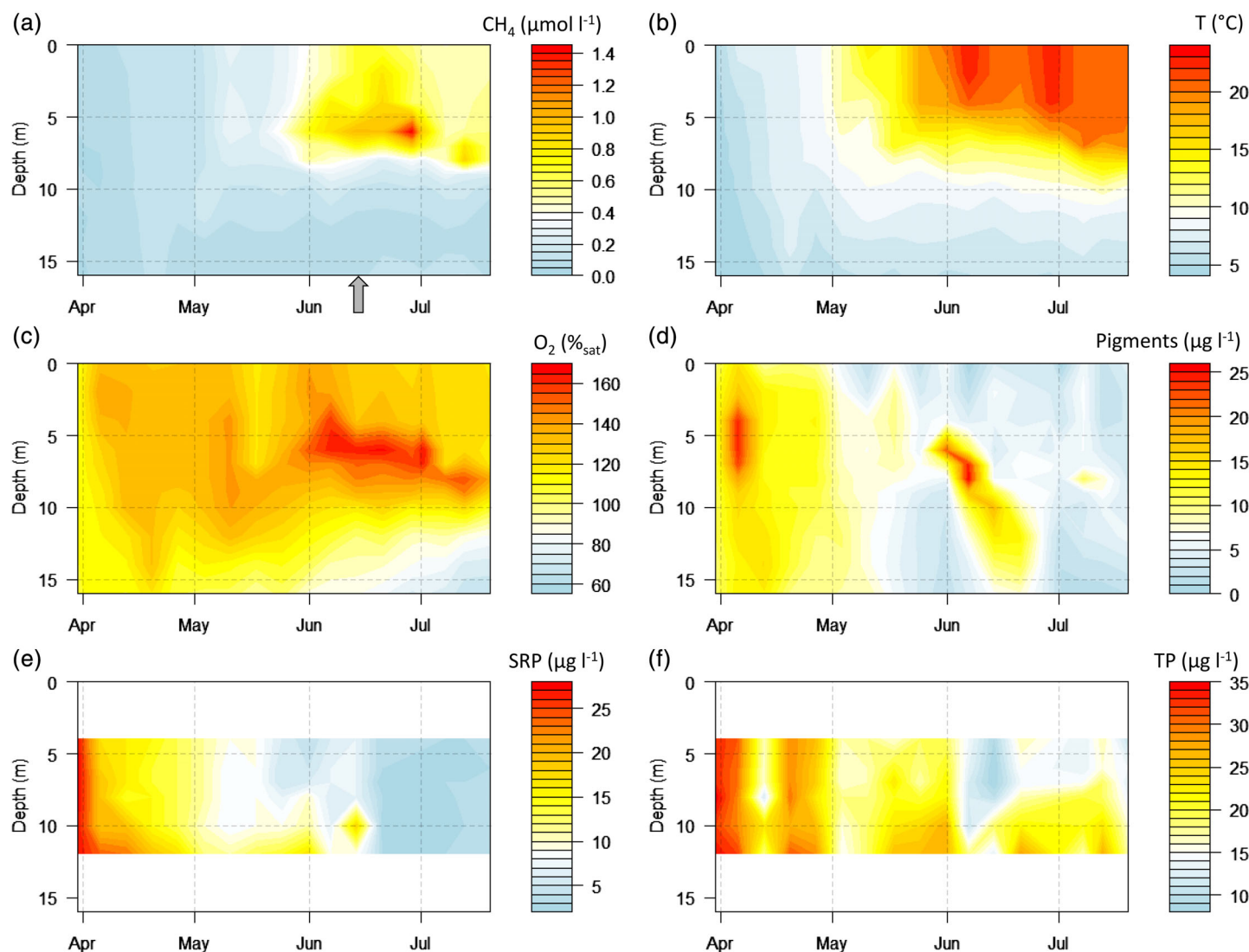


**Fig. 1.** Methane and environmental data—seasonal scale. (a) Methane concentration in  $\mu\text{mol L}^{-1}$ ; (b) temperature in  $^{\circ}\text{C}$ ; (c) oxygen saturation in %; (d) combined pigment concentration of green algae, cyanobacteria, diatoms, and cryptophytes in  $\mu\text{g L}^{-1}$ ; (e) SRP in  $\mu\text{g L}^{-1}$ ; and (f) total phosphorus (TP) in  $\mu\text{g L}^{-1}$ . Methane (a) and probe data (b–d) were recorded in the south basin and nutrient data in the northeast basin (e, f). The arrow marks the time point of water sampling for investigating depth-specific methane production rates.

concentrations and pigment concentrations of cyanobacteria ( $p < 0.001$ ), diatoms ( $p < 0.001$ , with temperature as interaction term), and cryptophytes ( $p \leq 0.04$ , with temperature as interaction term) at 0–20 m depth. Correlations are summarized in Supporting Information Table S1.

From the beginning of May to early June, the carbon isotope signature of water column  $\text{CH}_4$   $\delta^{13}\text{C}$  scattered around  $-50\text{‰}$  ( $\pm 2.5\text{‰}$ ) (Fig. 2a). In mid-June, the  $\delta^{13}\text{C}$  values increased to  $-45\text{‰}$  to  $-37\text{‰}$  (maximum at 7 m depth), then gradually decreased but remained greater than  $-50\text{‰}$  in July.

When plotted against SRP levels (Fig. 2b), both  $\delta^{13}\text{C}$  values ( $R^2 = 0.50$ ;  $p < 0.001$ ) and concentrations of  $\text{CH}_4$  ( $R^2 = 0.21$ ;  $p = 0.015$ ) showed negative correlations.

The water-to-air  $\text{CH}_4$  flux increased by an order of magnitude between March and July (Fig. 3a), and generally followed the increasing amount of  $\text{CH}_4$  in the upper 7 m (Fig. 1a), as well as increasing wind speed  $u_{10}$  (Supporting Information Fig. S4). Both  $\text{CH}_4$  accumulation and emission showed a negative log-linear relationship with SRP concentrations in the upper 7 m (Fig. 3b). Supporting Information

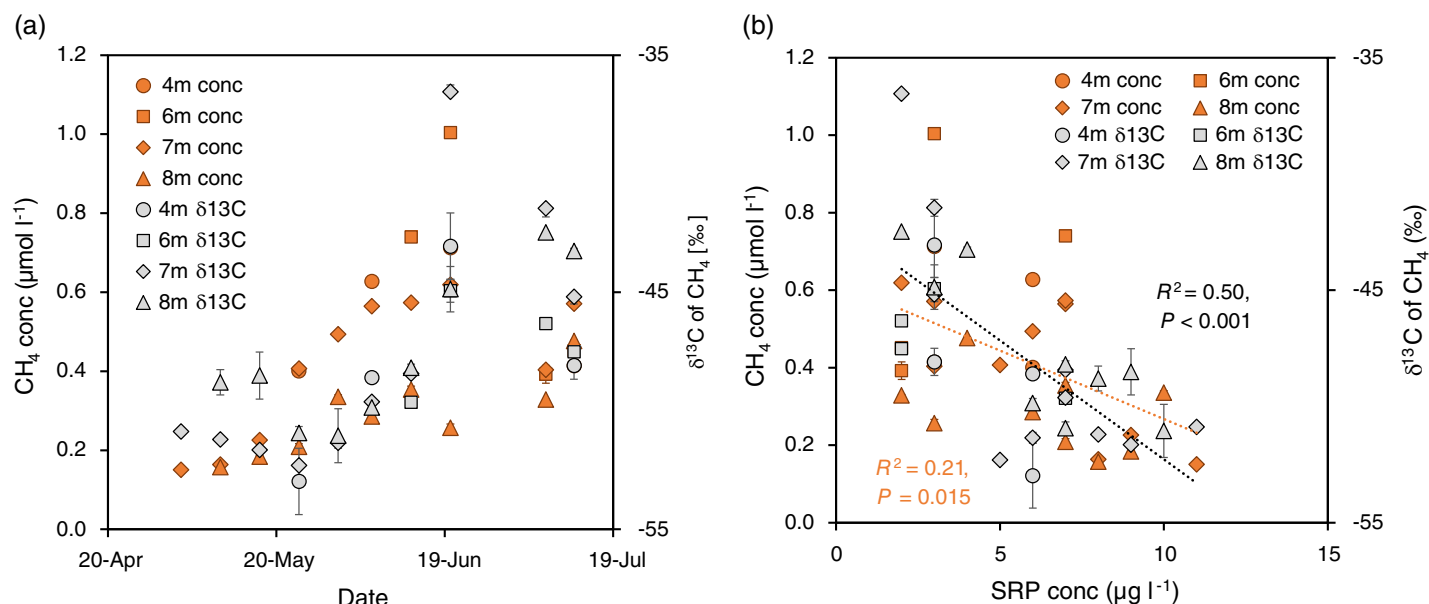


**Fig. 2.** Isotope characteristics of oxic methane accumulation. Methane concentrations and corresponding  $\delta^{13}\text{C}$  values in relation to (a) time and (b) ambient SRP concentrations.  $\text{CH}_4$  concentration ( $R^2 = 0.21$ ,  $p = 0.015$ ) and its  $^{13}\text{C}$  signature ( $R^2 = 0.50$ ,  $p < 0.001$ ) correlated negatively with SRP concentration ( $\text{CH}_4$  concentration/ $\delta^{13}\text{C}$ : mean  $\pm$  SD of triplicate measurements).

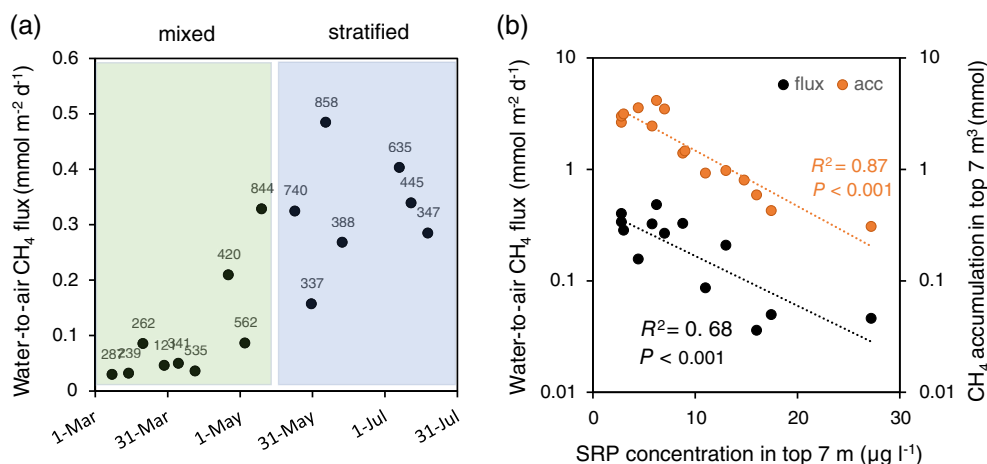


**Fig. 3.** Water-to-air  $\text{CH}_4$  flux and environmental parameters. Panel (a) shows the seasonal increase in surface emission. Data points are labeled with radiation values (combined direct solar and reflected/scattered radiation) recorded at 21 m height ( $\text{W m}^{-2}$ ). (b) Both surface emission ( $R^2 = 0.68$ ,  $p < 0.001$ ) and  $\text{CH}_4$  accumulation in the upper 7 m ( $R^2 = 0.87$ ,  $p < 0.001$ ) significantly increased with decreasing SRP concentration (upper 7 m) in a log-linear fashion. Note that y-axes in panel (b) are in log-scale.



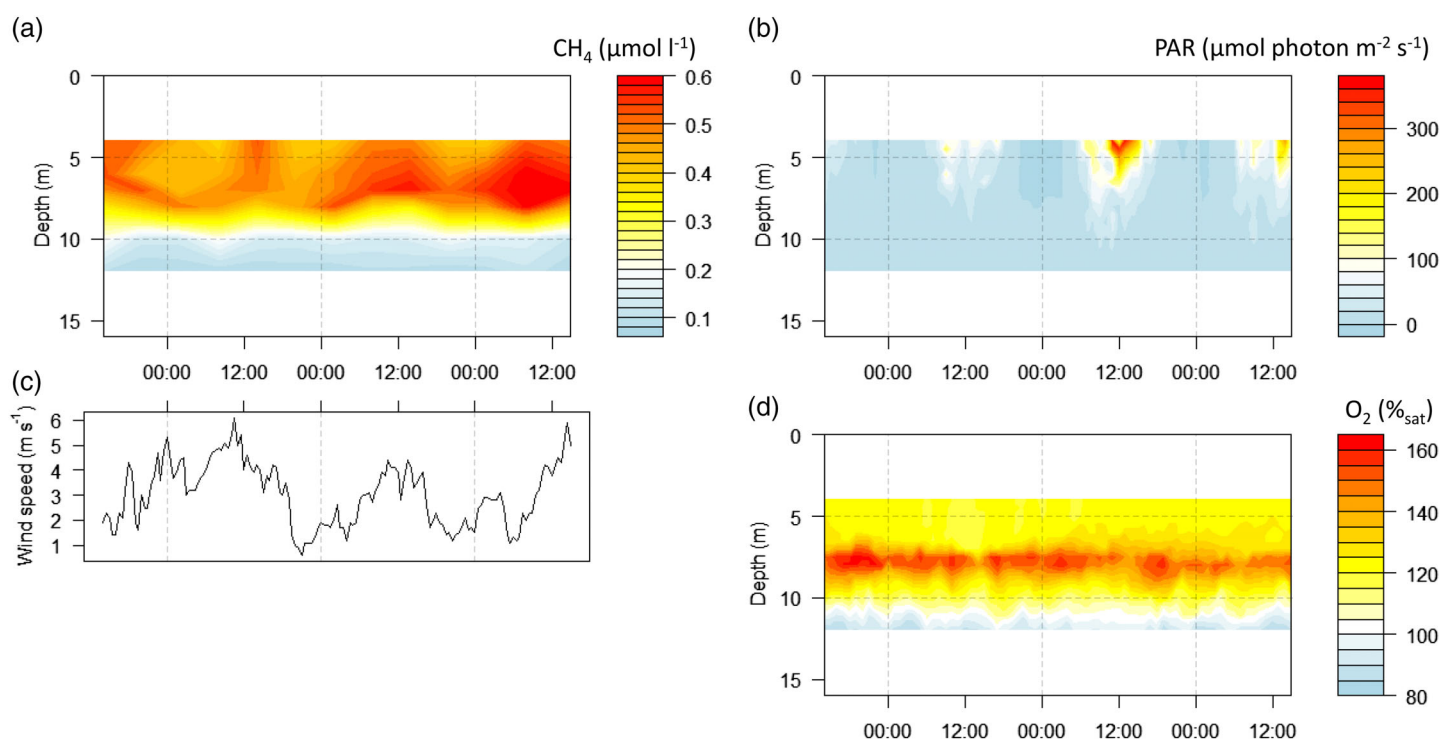


**Fig. 4.** Methane and environmental data—diurnal scale. **(a)** Methane concentration in  $\mu\text{mol L}^{-1}$ , **(b)** PAR in  $\mu\text{mol photons m}^{-2} \text{s}^{-1}$ , **(c)** wind speed  $u_{10}$  in  $\text{m s}^{-1}$  recorded at 10 m height, and **(d)** oxygen saturation in % throughout 8<sup>th</sup>–11<sup>th</sup> July 2016 in the south basin (24:00 h format; local time). The maximum diurnal  $\text{CH}_4$  concentration recorded was  $0.9 \mu\text{mol L}^{-1}$  during the last day of measurement at 08:00 h at 7 m depth, but the contour scale of panel **(a)** was limited to  $0.6 \mu\text{mol L}^{-1}$  to provide better resolution of the diurnal pattern.

Table S2 summarizes the seasonal surface flux data and related environmental data.

### Diurnal scale

Diurnal measurements revealed a rise-and-fall cycle of  $\text{CH}_4$  in the water column (Fig. 4a–d; Supporting Information Fig. S5). During daylight at about 10:00–14:00 h local time,  $\text{CH}_4$  concentrations increased to  $0.6$ – $0.9 \mu\text{mol L}^{-1}$ , whereas at night the concentrations dropped to about  $0.4 \mu\text{mol L}^{-1}$ . The highest daily  $\text{CH}_4$  accumulation coincided with the highest daily wind speeds around noon, showing variations in the  $\text{CH}_4$  inventory throughout a diurnal cycle. Strong  $\text{CH}_4$  accumulation consistently occurred at 7 m depth and at the  $16^\circ\text{C}$  isotherm, typically coinciding with high dissolved oxygen concentration (up to  $16 \text{ mg L}^{-1}$ ; 162% saturation). The  $\delta^{13}\text{C}$  values of  $\text{CH}_4$  at 7 m varied between  $-43\text{‰}$  and  $-47\text{‰}$  over the day–night cycle (Supporting Information Fig. S6). Similar to the seasonal data,  $\text{CH}_4$  showed a positive linear relationship with temperature ( $p < 0.001$ ), PAR ( $p = 0.003$ ), and oxygen saturation ( $p < 0.001$ ) throughout the diurnal cycle. To account for diurnal differences in fluorescence response, we analyzed the daytime (05:00–21:30 h) and nighttime phytoplankton pigment data (21:30–05:00 h) separately, both of which gave positive relationships between  $\text{CH}_4$  and chlorophyll (daytime:  $p = 0.002$ ; nighttime:  $p = 0.005$ ), green

algae (daytime:  $p < 0.001$ ; nighttime:  $p < 0.001$ ), cyanobacteria (daytime:  $p = 0.003$ ), and diatom pigment concentration (daytime:  $p = 0.02$ ; nighttime:  $p = 0.02$ ).

### Methane production by phytoplankton

#### Size fraction experiment

We measured  $\text{CH}_4$  production in the  $< 20 \mu\text{m}$  and  $> 20 \mu\text{m}$  size fractions of the lake water, as well as unfiltered lake water. The  $> 20 \mu\text{m}$  size fraction showed considerably higher net  $\text{CH}_4$  production (mean  $\pm$  SD) ( $19.2 \pm 0.9 \text{ nmol L}^{-1} \text{ d}^{-1}$ ) than the smaller fraction ( $4.3 \pm 0.3 \text{ nmol L}^{-1} \text{ d}^{-1}$ ) and unfiltered lake water ( $5.4 \pm 0.3 \text{ nmol L}^{-1} \text{ d}^{-1}$ ), suggesting that most of the  $\text{CH}_4$  production was associated with large phytoplankton cells, colonies, and particles (Fig. 5a). Microscopic observations revealed that cyanobacteria, diatoms, and green algae were prevalent in the  $> 20 \mu\text{m}$  size fraction (Supporting Information Fig. S2). In comparison,  $\text{CH}_4$  oxidation appeared to be primarily driven by cells smaller than  $20 \mu\text{m}$ .

#### Depth-specific methane production

Water samples collected in the epilimnion, thermocline, and hypolimnion (0–20 m sampled; ca. 20.5 m deep site) all showed increasing  $\text{CH}_4$  concentrations over time when incubated under natural daylight in the laboratory (Fig. 5b), and the highest production rates were found in waters collected

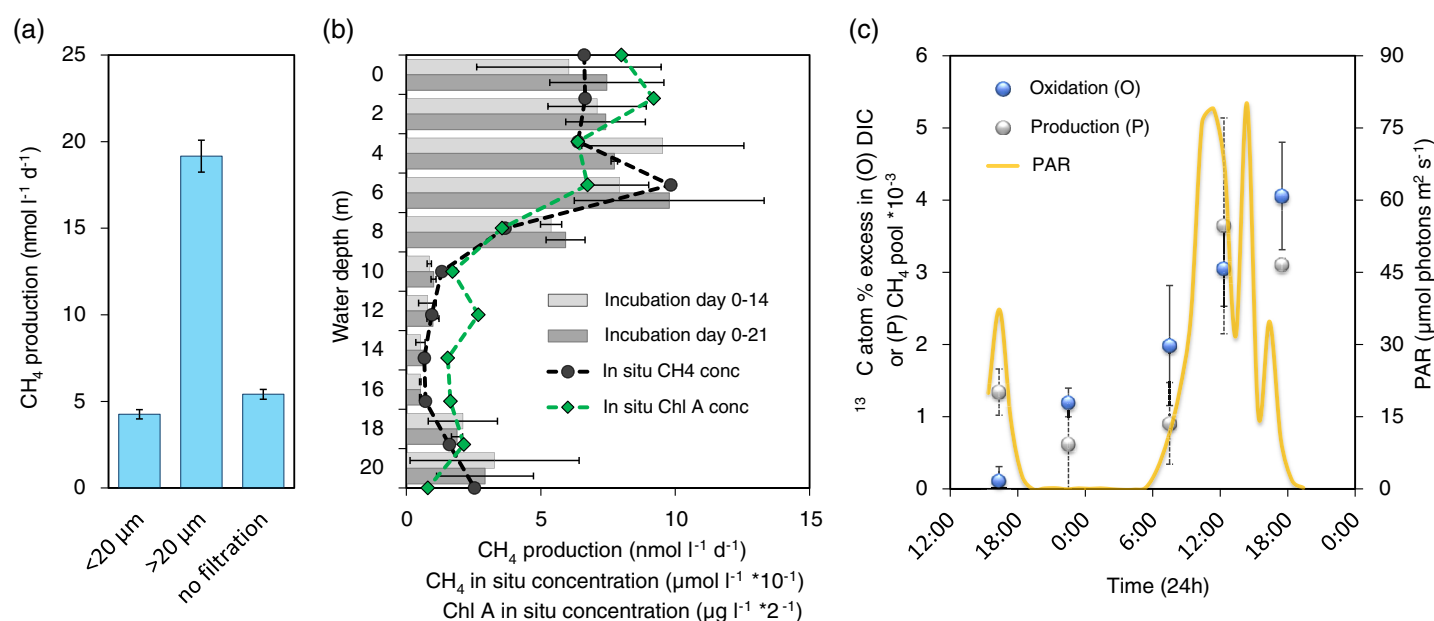


**Fig. 5.** Bottle incubation experiments. (a) Net CH<sub>4</sub> production rates of size-fractionated lake water vs. untreated lake water (mean  $\pm$  SD,  $n = 2$ ). (b) Depth-specific net CH<sub>4</sub> production rates (bars; mean  $\pm$  SD,  $n = 2$ ). The profile production rates mimic the profile of in situ CH<sub>4</sub> concentration (dotted symbols/line) and the profile of in situ Chl *a* concentration (green symbols/line). Note: for better illustration purpose, water samples taken from 7 and 9 m depth are not depicted (full data in Supporting Information Table S3). (c) CH<sub>4</sub> oxidation and CH<sub>4</sub> production as deduced from <sup>13</sup>C-label substrate turnover (oxidation: <sup>13</sup>CH<sub>4</sub>; production: DI<sup>13</sup>C) (mean  $\pm$  SD,  $n = 3$ ). Photosynthetically active radiation at ambient depth is symbolized by PAR. The average increasing <sup>13</sup>C excess over time in the DIC pool (= oxidation) had a positive linear slope ( $R^2 = 0.98$ ;  $p < 0.002$ ) whereas the average <sup>13</sup>C excess in the CH<sub>4</sub> pool (= production) did not show a significant linear slope ( $R^2 = 0.54$ ;  $p = 0.16$ ).

from the epilimnion and thermocline depth. Methane production was significantly correlated with in situ CH<sub>4</sub> concentration (incubation day 0–14:  $R^2 = 0.77$ ,  $p < 0.001$ ; incubation day 0–21:  $R^2 = 0.83$ ,  $p < 0.001$ ) and chlorophyll *a* (Chl *a*) concentration in the corresponding depths (incubation day 0–14:  $R^2 = 0.68$ ,  $p < 0.001$ ; incubation day 0–21:  $R^2 = 0.75$ ,  $p < 0.001$ ) (Supporting Information Table S3). Thus, waters collected from depths with high in situ CH<sub>4</sub> concentration showed high CH<sub>4</sub> production, and vice versa.

### <sup>13</sup>C labeling experiment

In this experiment, CH<sub>4</sub> oxidation and CH<sub>4</sub> production were measured using <sup>13</sup>C-labeled substrates and recording the incorporation of <sup>13</sup>C into the respective product pools over time. Thermocline-depth water samples treated with <sup>13</sup>CH<sub>4</sub> showed a linear increase in incorporation of <sup>13</sup>C into the DIC pool over time (Fig. 5c), whereas samples treated with methyl fluoride to inhibit CH<sub>4</sub> oxidation showed negligible change in DI<sup>13</sup>C. The difference between the two treatments gave a CH<sub>4</sub> oxidation of  $1.9 \pm 0.3$  pmol L<sup>-1</sup> h<sup>-1</sup> (Eq. 1). In the parallel treatment groups, the addition of NaH<sup>13</sup>CO<sub>3</sub> resulted in incorporation of <sup>13</sup>C into the CH<sub>4</sub> pool (Fig. 5c). There was a small decrease in the <sup>13</sup>CH<sub>4</sub> pool at night even with added methyl fluoride, suggesting incomplete inhibition of CH<sub>4</sub> oxidation, whereas <sup>13</sup>C incorporation into CH<sub>4</sub> during daytime exceeded the nighttime loss. Based on <sup>13</sup>C incorporation, the net change in CH<sub>4</sub> varied between  $-1.4$  (night) and  $7$  pmol L<sup>-1</sup> h<sup>-1</sup>

(day) throughout the diurnal cycle (Fig. 5c). Using Eq. 2 and applying the average oxidation rate from the <sup>13</sup>CH<sub>4</sub> labeling experiment, the gross CH<sub>4</sub> production was estimated to be  $0.5$  (night) and  $8.9$  pmol L<sup>-1</sup> h<sup>-1</sup> (day). The results are summarized in Supporting Information Tables S4 and S5.

### Phosphorus addition experiment

An integrated lake water sample was taken from 4 to 8 m depth during the stratified and phosphorus limited season ( $\text{SRP} \leq 3 \mu\text{g L}^{-1}$ ) (Supporting Information Fig. S7). This lake water was incubated in the laboratory under natural daylight exposure or in darkness, with or without the addition of K<sub>2</sub>HPO<sub>4</sub>. All treatment groups remained oxic throughout the experiment and  $\delta^{13}\text{C}$  values varied among the treatment groups (Supporting Information Fig. S8 and Table S6). While the addition of phosphorus shifted  $\delta^{13}\text{C}$  to more negative values in the light treatment, dark incubation resulted in more positive  $\delta^{13}\text{C}$  values.

### Pure culture experiment

Both the freshwater diatom *Navicula* sp. and the marine diatom *Leptocylindrus danicus* showed CH<sub>4</sub> production (Fig. 6). Highest CH<sub>4</sub> production rates were observed during the light periods, especially during highest light intensities. During dark phases production rates were low (both species) or undetectable (*Navicula* sp.). A decrease in CH<sub>4</sub> concentration could be the result of either decreased or no production coupled with degassing from the supersaturated, continuously



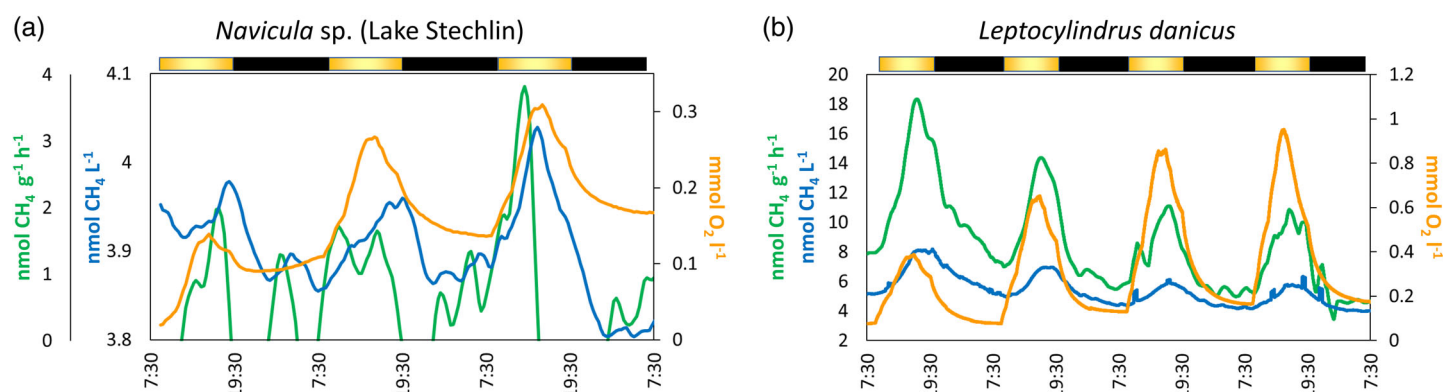


**Fig. 6.** Pure culture experiments. Membrane inlet mass spectrometry (MIMS) was deployed to record methane and oxygen throughout incubation of (a) the freshwater diatom *Navicula* sp. (isolated from Lake Stechlin), and (b) the marine diatom *Leptocylindrus danicus*. The blue line resembles methane concentration, the green line is methane production normalized to dry weight, and the yellow line is the oxygen concentration inside the experimental MIMS chamber. A Savitzky-Golay filter (20 min interval) was applied to remove outlier data points. The light regime for the experiments was as follows: dark (black bar) from 19:30 h to 09:00 h then light intensity was programmed to increase to 60, 120, 180, and 400  $\mu\text{mol photon m}^{-2} \text{ s}^{-1}$  with a hold time of 1.5 h at each intensity (yellow to white bar). After maximum light period, the intensity was programmed to decrease in reverse order with the same hold times until complete darkness again at 19:30 h.

mixing, semi-closed incubation chamber toward equilibrium with atmospheric  $\text{CH}_4$  ( $2.5 \text{ nmol L}^{-1}$  and  $2.1 \text{ nmol L}^{-1}$  for freshwater and seawater, respectively).

## Discussion

### Environmental setting

Methane accumulation in oxic surface waters of temperate lakes often coincides with seasonal stratification (Bastviken et al. 2008; Tang et al. 2016). In our study,  $\text{CH}_4$  concentrations were up to 115 times higher in the summer months than in early spring, leading to a 29-fold increase in total  $\text{CH}_4$  in the top 7 m of the strongly oxygenated water column ( $> 100\%$  saturation;  $> 10 \text{ mg L}^{-1}$ ) between late March and July.

While it is common to describe  $\text{CH}_4$  dynamics based on either exclusively  $\text{CH}_4$  concentration data (e.g., Juutinen et al. 2009; Li et al. 2018) or exclusively  $\text{CH}_4$  isotope data (e.g., Cadieux et al. 2016; Lecher et al. 2017), by combining both data types we revealed a new aspect of  $\text{CH}_4$  dynamics in the water column. For example, when considering  $\text{CH}_4$  concentration alone, the increase in in situ mid-water  $\text{CH}_4$  between March and July (Fig. 2a) can be interpreted as the result of a stronger or accumulating  $\text{CH}_4$  input from sediments and littoral zone, which would be accompanied by a decrease in the corresponding  $\delta^{13}\text{C}$  value indicative of anoxic  $\text{CH}_4$  (Whiticar 1999). Conversely, when only considering  $\text{CH}_4$  isotope data alone, the observed  $^{13}\text{C}$  enrichment throughout June (Fig. 2a) can be interpreted as an increase in  $\text{CH}_4$  oxidation activity, which should also lead to a decrease in the corresponding  $\text{CH}_4$  concentration (Whiticar 1999). However, by combining both data sets we showed a concurrent increase in both  $\text{CH}_4$  concentration (from ca.  $0.3/0.6$  to  $1.0 \mu\text{mol L}^{-1}$ ) and  $\delta^{13}\text{C}$  signature (from ca.  $-52\text{‰}$  to  $-37\text{‰}$ ). Our

observations allow the alternative explanation of an internal (oxic)  $\text{CH}_4$  source with a  $\delta^{13}\text{C}$  signature distinctively higher than that of the anoxic  $\text{CH}_4$  sources. This explanation is supported by our bottle incubations showing active  $\text{CH}_4$  production under oxic conditions, and a recent study modeling  $\text{CH}_4$  carbon isotope changes in lake water (Hartmann et al. 2020).

Phosphorus deficiency has been shown to promote demethylation of MPNs with subsequent  $\text{CH}_4$  release in both marine and freshwater environments (Carini et al. 2014; Repeta et al. 2016; Yao et al. 2016; Wang et al. 2017). Methyl groups cleaved from the C-1 compounds are converted to  $\text{CH}_4$  by a reductase, potentially drawing the required reductive power via electron dumping from photosynthesis (Tang et al. 2014), especially under nutrient limitation (Hemschemeier and Happe 2011). This hypothesis is corroborated by our field and lab measurements together showing that oxic  $\text{CH}_4$  production was connected to photosynthesis as well as low SRP concentrations. Nevertheless, it remains unclear whether the MPN pathway would result in  $\text{CH}_4$  with  $\delta^{13}\text{C}$  values greater than  $-40\text{‰}$  (kinetic isotope effects strongly depend on elemental composition and molecule configuration; therefore, incubation experiments with enriched MPN pool as  $\text{CH}_4$  precursor do not reflect the natural  $\delta^{13}\text{C}$  response in the field).

### Methane production by phytoplankton

Several lines of evidence point to the direct role of phytoplankton in oxic  $\text{CH}_4$  production in our study. First, in situ  $\text{CH}_4$  concentrations were positively correlated to PAR, phytoplankton pigment concentrations, and oxygen (over)saturation (as a by-product of photosynthesis). Second, our diurnal measurements showed a cyclical  $\text{CH}_4$  pattern in the water

column that aligned with the light–dark periods. Third, highest CH<sub>4</sub> production was observed in the > 20 µm size fraction, which contained mostly cyanobacteria, diatoms, and green algae. Our light incubations using lake water amended with K<sub>2</sub>HPO<sub>4</sub> resulted in a δ<sup>13</sup>C shift toward more negative values, whereas dark incubation resulted in more positive values, together indicating that CH<sub>4</sub> production was triggered by light. The alternative explanation of light-inhibited CH<sub>4</sub> oxidation (Murase and Sugimoto 2005) is unlikely to be relevant because our <sup>13</sup>C-labeling experiment showed constant oxidation rates throughout the diurnal cycle (Fig. 4c). Further direct evidence was provided by incubation with NaH<sup>13</sup>CO<sub>3</sub> resulting in a much higher incorporation of <sup>13</sup>C into CH<sub>4</sub> in daytime vs. nighttime, showing that photoautotrophic carbon fixation was involved in the process, as we hypothesized earlier (Tang et al. 2014). Among the major phytoplankton groups, cyanobacteria showed the strongest and most consistent positive correlation with CH<sub>4</sub> concentrations in situ, implicating their key role in oxic CH<sub>4</sub> production. Using cyanobacteria cultures and a MIMS, Bizic et al. (2020) showed that CH<sub>4</sub> production follows the light–dark cycle with a small time-lag. Here, we conducted similar MIMS measurements with cultures of the freshwater diatom *Navicula* sp. (isolated from Lake Stechlin) and the marine diatom *Leptocylindrus danicus* (Fig. 6). Both species showed CH<sub>4</sub> production aligning with light–dark incubation periods and more CH<sub>4</sub> was produced at higher light intensities. Combining ours and others' findings (Bizic et al. 2020; Hartmann et al. 2020), the results suggest that light-triggered CH<sub>4</sub> production may be common among phytoplankton. It is likely that the conversion of NaH<sup>13</sup>CO<sub>3</sub> to CH<sub>4</sub> involves multiple steps, not all being light-dependent (decreased but active CH<sub>4</sub> production during dark phases: Bizic et al. 2020; Fig. 6). Nevertheless, the observations that oxic CH<sub>4</sub> production was linked to photosynthesis indicate that the oxic and anoxic methane sources will react differently to environmental perturbations.

In the marine environment, the cyanobacterium *Trichodesmium erythraeum* has been found to carry gene cassettes encoding the enzymes for the conversion of MPNs to CH<sub>4</sub> (Dyhrman et al. 2006; Beversdorf et al. 2010). Similar genes have been found in the freshwater cyanobacterium *Picocyanobacterium* (Kutovaya et al. 2013; Yao et al. 2016). However, in previous studies, enrichment of Lake Stechlin water with MPNs has produced conflicting results in stimulating CH<sub>4</sub> production (Grossart et al. 2011; Bizic-Ionescu et al. 2018). Another possible pathway involves nitrogenase enzymes, which are common among cyanobacteria (Bothe et al. 2010). Iron-only nitrogenases of wild-type proteobacteria have been shown to convert carbon dioxide, nitrogen gas and protons to CH<sub>4</sub> in a single enzymatic reaction, and the CH<sub>4</sub> yield increases with increasing light intensity (up to 30 µmol photons m<sup>-2</sup> s<sup>-1</sup>) (Zheng et al. 2018). Furthermore, this reaction has been found in an obligate aerobic bacterium, *Azotobacter vinelandii* (Zheng et al. 2018). However, the iron-

only nitrogenase activity has never been demonstrated in CH<sub>4</sub> production by cyanobacteria. Diatoms are generally incapable of nitrogen-fixation; therefore, the observed CH<sub>4</sub> production (Fig. 6) indicates that the underlying mechanism does not necessarily require nitrogenase.

### Implication for methane emission to the atmosphere

Measured net CH<sub>4</sub> production was comparable above and within the thermocline; loss of CH<sub>4</sub> to oxidation and diffusion within the epilimnion could result in a concentration gradient with the CH<sub>4</sub> maximum at the thermocline as observed. An earlier study did not detect more methane oxidizer in surface water compared to thermocline water (Grossart et al. 2011); therefore, it is more likely that the gradient was caused by diffusive loss of CH<sub>4</sub> across the water–air interface, which is corroborated by our surface flux measurements. To explain the observed average surface flux of 0.32 mmol m<sup>-2</sup> d<sup>-1</sup> during the stratified season (after 17<sup>th</sup> May), it would require an oxic production of 46 nmol L<sup>-1</sup> d<sup>-1</sup> in the upper 7 m. In our incubation experiment, water collected from the upper 7 m yielded about 8 nmol L<sup>-1</sup> d<sup>-1</sup> oxic CH<sub>4</sub> production. Our measurement represents only a snapshot of the system and does not fully capture the natural variability of CH<sub>4</sub> production. For example, Grossart et al. (2011) reported about seven times higher oxic CH<sub>4</sub> production rate in an earlier year based on bottle incubations. Günthel et al. (2019) and Hartmann et al. (2020), using mass balance analysis of CH<sub>4</sub> production and loss, arrived at oxic CH<sub>4</sub> production rates of up to > 200 nmol L<sup>-1</sup> d<sup>-1</sup>. Therefore, our oxic CH<sub>4</sub> production rates should be considered conservative, which potentially explained 18% of the observed average surface flux. Similarly, recent investigations in the mesotrophic Lake Hallwil, Switzerland found that about 63–90% of CH<sub>4</sub> emission could be attributed to oxic CH<sub>4</sub> production and accumulation in the upper mixed layer (Donis et al. 2017; Günthel et al. 2019). Light and phosphorus were found in our incubation experiments to be important factors for oxic CH<sub>4</sub> production, which is consistent with our field observations that the water-to-air CH<sub>4</sub> flux correlates with both parameters. Together, our observations suggest that oxic CH<sub>4</sub> production in the upper layer is an important contributor to CH<sub>4</sub> emission, but hitherto has not been acknowledged in global methane budgets and models (IPCC 2013).

### Reconsidering the methane paradox

The methane paradox is rooted in the paradigm that biological CH<sub>4</sub> production occurs strictly under anoxic conditions and therefore, oxic-water CH<sub>4</sub> oversaturation is often exclusively attributed to physical transport from anoxic sources. However, reports of oxic CH<sub>4</sub> production by terrestrial flora and fauna have prompted questions of this paradigm (Keppler et al. 2006; Ghyczy et al. 2008; Lenhart et al. 2012; Althoff et al. 2014). Similarly, the mounting evidence in both marine and freshwater environments (Tang et al. 2016) and reference therein,

including this study, has demonstrated unequivocally that active biological CH<sub>4</sub> production occurs in oxic waters. Accordingly, the methane paradox can be explained, at least partially, by internal oxic production (Grossart et al. 2011; Tang et al. 2014; Günthel et al. 2019), with or without external inputs (Fernandez et al. 2016; DelSontro et al. 2018; Peeters et al. 2019).

Pure-culture experiments demonstrated the ability of oxic CH<sub>4</sub> production in diatoms (Hartmann et al. 2020; this study), cyanobacteria (Bizic et al. 2020), green algae, and cryptophytes (Hartmann et al. 2020). Additionally, our study showed the conversion of (<sup>13</sup>C-labeled) bicarbonate to CH<sub>4</sub> demonstrating a direct link of oxic CH<sub>4</sub> production to photosynthesis, and our field data corroborate the involvement of diatoms, cyanobacteria, green algae, and cryptophytes. While the precise biochemical pathway(s) is subject to further investigation, these findings together indicate CH<sub>4</sub> production may be a common feature among diverse phytoplankton taxa. Phytoplankton are ubiquitous in illuminated aquatic environments and are globally on the rise (Hampton et al. 2008; Duan et al. 2009; Ho et al. 2019). It is therefore necessary to understand how these potential oxic methane producers react to environmental perturbation such as widespread eutrophication and global warming, and the corresponding effect on atmospheric CH<sub>4</sub> emission. Available data for Lake Stechlin (Günthel et al. 2019, Hartmann et al. 2020; this study), Lake Cromwell (Bogard et al. 2014) and Lake Hallwil (Donis et al. 2017, Günthel et al. 2019) show that oxic CH<sub>4</sub> production can account for 18–90% of the surface emission. Albeit limited, these findings warrant an urgent re-examination of the (aquatic) CH<sub>4</sub> cycle (Kirschke et al. 2013; Saunio et al. 2016) and climate change predictions (IPCC 2013) that are presently based on almost exclusively conventional anoxic CH<sub>4</sub> sources.

#### Data availability statement

Manuscript related data are available in tabular form in the Supporting Information (incubation experiments, flux data) and via GLEON data repositories upon acceptance (seasonal and diurnal field data) (<http://gleon.org/>).

#### References

- Abell, J. M., D. Özkundakci, and D. P. Hamilton. 2010. Nitrogen and phosphorus limitation of phytoplankton growth in New Zealand lakes: Implications for eutrophication control. *Ecosystems* **13**: 966–977. doi:[10.1007/s10021-010-9367-9](https://doi.org/10.1007/s10021-010-9367-9)
- Althoff, F., K. Benzing, P. Comba, C. McRoberts, D. R. Boyd, S. Greiner, and F. Keppler. 2014. Abiotic methanogenesis from organosulphur compounds under ambient conditions. *Nat. Commun.* **5**: 4205. doi:[10.1038/ncomms5205](https://doi.org/10.1038/ncomms5205)
- Bastviken, D., J. J. Cole, M. L. Pace, and M. C. Van de Bogert. 2008. Fates of methane from different lake habitats: Connecting whole-lake budgets and CH<sub>4</sub> emissions. *J. Geophys. Res. Biogeosci.* **113**: 1–13. doi:[10.1029/2007JG000608](https://doi.org/10.1029/2007JG000608)
- Beversdorf, L. J., A. E. White, K. M. Björkman, R. M. Letelier, and D. M. Karl. 2010. Phosphonate metabolism by *Trichodesmium* IMS101 and the production of greenhouse gases. *Limnol. Oceanogr.* **55**: 1768–1778. doi:[10.4319/lo.2010.55.4.1768](https://doi.org/10.4319/lo.2010.55.4.1768)
- Bizic, M., and others. 2020. Aquatic and terrestrial cyanobacteria produce methane. *Sci. Adv.* **6**: eaax5343. doi:[10.1126/sciadv.aax5343](https://doi.org/10.1126/sciadv.aax5343)
- Bizic-Ionescu, M., D. Ionescu, M. Günthel, K. W. Tang, and H.-P. Grossart. 2018. Oxic methane cycling: New evidence for methane formation in oxic lake water, p. 1–22. In J. M. Alfons and D. Sousa [eds.], *Biogenesis of hydrocarbons*. Springer.
- Bogard, M., P. A. del Giorgio, L. Boutet, M. C. Garcia-Chaves, Y. T. Prairie, A. Merante, and A. M. Derry. 2014. Oxic water column methanogenesis as a major component of aquatic CH<sub>4</sub> fluxes. *Nat. Commun.* **5**: 5350. doi:[10.1038/ncomms6350](https://doi.org/10.1038/ncomms6350)
- Bothe, H., O. Schmitz, M. G. Yates, and W. E. Newton. 2010. Nitrogen fixation and hydrogen metabolism in cyanobacteria. *Microbiol. Mol. Biol. Rev.* **74**: 529–551. doi:[10.1128/MMBR.00033-10](https://doi.org/10.1128/MMBR.00033-10)
- Cadieux, S. B., J. R. White, P. E. Sauer, Y. Peng, A. E. Goldman, and L. M. Pratt. 2016. Large fractionations of C and H isotopes related to methane oxidation in Arctic lakes. *Geochim. Cosmochim. Acta* **187**: 141–155. doi:[10.1016/j.gca.2016.05.004](https://doi.org/10.1016/j.gca.2016.05.004)
- Carini, P., A. E. White, E. O. Campbell, and S. J. Giovannoni. 2014. Methane production by phosphate-starved SAR11 chemoheterotrophic marine bacteria. *Nat. Commun.* **5**: 4346. doi:[10.1038/ncomms5346](https://doi.org/10.1038/ncomms5346)
- Casper, S. J. 1985. *Lake Stechlin: A temperate oligotrophic lake*. Dr W. Junk Publishers.
- Chan, A. S. K., and T. B. Parkin. 2000. Evaluation of potential inhibitors of methanogenesis and methane oxidation in a landfill cover soil. *Soil Biol. Biochem.* **32**: 1581–1590. doi:[10.1016/S0038-0717\(00\)00071-7](https://doi.org/10.1016/S0038-0717(00)00071-7)
- Conrad, R., O.-C. Chan, P. Claus, and P. Casper. 2007. Characterization of methanogenic Archaea and stable isotope fractionation during methane production in the profundal sediment of an oligotrophic lake (Lake Stechlin, Germany). *Limnol. Oceanogr.* **52**: 1393–1406. doi:[10.4319/lo.2007.52.4.1393](https://doi.org/10.4319/lo.2007.52.4.1393)
- Damm, E., E. Helmke, S. Thoms, U. Schauer, E. Nöthig, K. Bakker, and R. P. Kiene. 2010. Methane production in aerobic oligotrophic surface water in the central Arctic Ocean. *Biogeosciences* **7**: 1099–1108. doi:[10.5194/bg-7-1099-2010](https://doi.org/10.5194/bg-7-1099-2010)
- Dean, J. F., and others. 2018. Methane feedbacks to the global climate system in a warmer world. *Rev. Geophys.* **56**: 207–250. doi:[10.1002/2017RG000559](https://doi.org/10.1002/2017RG000559)
- DelSontro, T., P. A. del Giorgio, and Y. T. Prairie. 2018. No longer a paradox: The interaction between physical transport and biological processes explains the spatial

- distribution of surface water methane within and across lakes. *Ecosystems* **21**: 1073–1087. doi:[10.1007/s10021-017-0205-1](https://doi.org/10.1007/s10021-017-0205-1)DO
- Donis, D., S. Flury, A. Stöckli, J. E. Spangenberg, D. Vachon, and D. F. McGinnis. 2017. Full-scale evaluation of methane production under oxic conditions in a mesotrophic lake. *Nat. Commun.* **8**: 1661. doi:[10.1038/s41467-017-01648-4](https://doi.org/10.1038/s41467-017-01648-4)DO
- Duan, H., R. Ma, X. Xu, F. Kong, S. Zhang, W. Kong, J. Hao, and L. Shang. 2009. Two-decade reconstruction of algal blooms in China's Lake Taihu. *Environ. Sci. Technol.* **43**: 3522–3528. doi:[10.1021/es8031852](https://doi.org/10.1021/es8031852)
- Dyrhman, S. T., P. D. Chappell, S. T. Haley, J. W. Moffett, E. D. Orchard, J. B. Waterbury, and E. A. Webb. 2006. Phosphonate utilization by the globally important marine diazotroph *Trichodesmium*. *Nature* **439**: 68–71. doi:[10.1038/nature04203](https://doi.org/10.1038/nature04203)DO
- Fernandez, J. E., F. Peeters, and H. Hofmann. 2016. On the methane paradox: Transport from shallow water zones rather than in situ methanogenesis is the major source of CH<sub>4</sub> in the open surface water of lakes. *J. Geophys. Res. Biogeosci.* **121**: 2717–2726. doi:[10.1002/2016JG003586](https://doi.org/10.1002/2016JG003586)
- Ferry, J. G., and K. A. Kestead. 2007. Methanogenesis, p. 288–314. *In* R. Cavicchioli [ed.], *Archae: Molecular and cellular biology*. ASM Press.
- Ghyrczy, M., C. Torday, J. Kaszaki, A. Szabó, M. Czóbel, and M. Boros. 2008. Hypoxia-induced generation of methane in mitochondria and eukaryotic cells - an alternative approach to methanogenesis. *Cell Physiol. Biochem.* **21**: 251–258. doi:[10.1159/000113766](https://doi.org/10.1159/000113766)
- Grossart, H.-P., K. Frindte, C. Dzallas, W. Eckert, and K. W. Tang. 2011. Microbial methane production in oxygenated water column of an oligotrophic lake. *Proc. Natl. Acad. Sci. USA* **108**: 19657–19661. doi:[10.1073/pnas.110716108](https://doi.org/10.1073/pnas.110716108)
- Guildford, S. J., H. A. Bootsma, E. J. Fee, R. E. Hecky, and G. Patterson. 2000. Phytoplankton nutrient status and mean water column irradiance in Lakes Malawi and Superior. *Aquat. Ecosyst. Health Manag.* **3**: 35–45. doi:[10.1080/14634980008656989](https://doi.org/10.1080/14634980008656989)
- Günthel, M., D. Donis, G. Kirillin, D. Ionescu, M. Bizic, D. F. McGinnis, H.-P. Grossart, and K. W. Tang. 2019. Contribution of oxic methane production to surface methane emission in lakes and its global importance. *Nat. Commun.* **10**: 5497. doi:[10.1038/s41467-019-13320-0](https://doi.org/10.1038/s41467-019-13320-0)
- Hampton, S., L. R. Izmet'eva, M. V. Morre, S. L. Katz, B. Dennis, and E. A. Silow. 2008. Sixty years of environmental change in the world's largest freshwater lake – Lake Baikal, Siberia. *Glob. Chang. Biol.* **14**: 1947–1958. doi:[10.1111/j.1365-2486.2008.01616.x](https://doi.org/10.1111/j.1365-2486.2008.01616.x)
- Hartmann, J. F., M. Günthel, T. Klitzsch, G. Kirillin, H.-P. Grossart, F. Keppler, and M. Isenbeck-Schröter. 2020. High spatiotemporal dynamics of methane production and emission in oxic surface water. *Environ. Sci. Technol.* **54**: 1451–1463. doi:[10.1021/acs.est.9b03182](https://doi.org/10.1021/acs.est.9b03182)
- Hemschemeier, A., and T. Happe. 2011. Alternative photosynthetic electron transport pathways during anaerobiosis in the green alga *Chlamydomonas reinhardtii*. *Biochim. Biophys. Acta* **1807**: 919–926. doi:[10.1016/j.bbabi.2011.02.010](https://doi.org/10.1016/j.bbabi.2011.02.010)
- Ho, J. C., A. M. Michalak, and N. Pahlevan. 2019. Widespread global increase in intense lake phytoplankton blooms since the 1980s. *Nature* **574**: 667–670. doi:[10.1038/s41586-019-1648-7](https://doi.org/10.1038/s41586-019-1648-7)
- IPCC. 2013. *Climate Change 2013: The physical science basis. Contribution of working group I to the fifth assessment report of the Intergovernmental Panel on Climate Change*. Cambridge Univ. Press.
- Juutinen, S., M. Rantakari, P. Kortelainen, J. T. Huttunen, T. Larmola, J. Alm, J. Silvola, and P. J. Martikainen. 2009. Methane dynamics in different boreal lake types. *Biogeosciences* **6**: 209–223. doi:[10.5194/bg-6-209-2009](https://doi.org/10.5194/bg-6-209-2009)
- Kana, T. M., J. C. Cornwell, and L. Zhong. 2006. Determination of denitrification in the Chesapeake Bay from measurements of N<sub>2</sub> accumulation in bottom water. *Estuaries Coast.* **29**: 222–231.
- Karl, D. M., L. Beversdorf, K. M. Björkman, M. J. Church, A. Martinez, and E. F. Delong. 2008. Aerobic production of methane in the sea. *Nat. Geosci.* **1**: 473–478. doi:[10.1038/ngeo234](https://doi.org/10.1038/ngeo234)
- Keppler, F., J. T. G. Hamilton, M. Braß, and T. Röckmann. 2006. Methane emissions from terrestrial plants under aerobic conditions. *Nature* **439**: 187–191. doi:[10.1038/nature04420](https://doi.org/10.1038/nature04420)DO
- Khatun, S., and others. 2019. Aerobic methane production by planktonic microbes in lakes. *Sci. Total Environ.* **696**: 133916. doi:[10.1016/j.scitotenv.2019.133916](https://doi.org/10.1016/j.scitotenv.2019.133916)
- Kirschke, S., and others. 2013. Three decades of global methane sources and sinks. *Nat. Geosci.* **6**: 813–823. doi:[10.1038/ngeo1955](https://doi.org/10.1038/ngeo1955)
- Klitzsch, T., G. Langer, G. Nehrke, A. Wieland, K. Lenhart, and F. Keppler. 2019. Methane production by three widespread marine phytoplankton species: Release rates, precursor compounds, and relevance for the environment. *Biogeosciences* **16**: 4129–4144. doi:[10.5194/bg-16-4129-2019-245](https://doi.org/10.5194/bg-16-4129-2019-245)
- Kutovaya, O. A., R. M. L. McKay, and G. S. Bullerjahn. 2013. Detection and expression of genes for phosphorus metabolism in picocyanobacteria from the Laurentian Great Lakes. *J. Great Lakes Res.* **39**: 612–621. doi:[10.1016/j.jglr.2013.09.009](https://doi.org/10.1016/j.jglr.2013.09.009)
- Lecher, A. L., P.-C. Chuang, M. Singleton, and A. Paytan. 2017. Sources of methane to an Arctic lake in Alaska: An isotope investigation. *J. Geophys. Res. Biogeosci.* **122**: 753–766. doi:[10.1002/2016JG003491](https://doi.org/10.1002/2016JG003491)
- Lenhart, K., and others. 2012. Evidence for methane production by saprotrophic fungi. *Nat. Commun.* **3**: 1046. doi:[10.1038/ncomms2049](https://doi.org/10.1038/ncomms2049)
- Lenhart, K., T. Klitzsch, G. Langer, G. Nehrke, M. Bunge, S. Schnell, and F. Keppler. 2016. Evidence for methane production by the marine algae *Emiliania huxleyi*. *Biogeosciences* **13**: 3163–3174. doi:[10.5194/bg-13-3163-2016](https://doi.org/10.5194/bg-13-3163-2016)



- Li, L., B. Xue, S. Yao, Y. Tao, and R. Yan. 2018. Spatial-temporal patterns of methane dynamics in Lake Taihu. *Hydrobiologia* **822**: 143–156. doi:[10.1007/s10750-018-3670-4](https://doi.org/10.1007/s10750-018-3670-4)
- Lyu, Z., and Y. Liu. 2019. Diversity and taxonomy of methanogens, p. 1–22. *In* J. M. Alfons and D. Sousa [eds.], *Bio-genesis of hydrocarbons*. Springer.
- Murase, J., and A. Sugimoto. 2005. Inhibitory effect of light on methane oxidation in the pelagic water column of a mesotrophic lake (Lake Biwa, Japan). *Limnol. Oceanogr.* **50**: 1339–1343. doi:[10.4319/lo.2005.50.4.1339](https://doi.org/10.4319/lo.2005.50.4.1339)
- Peeters, F., J. E. Fernandez, and H. Hofmann. 2019. Sediment fluxes rather than oxic methanogenesis explain diffusive CH<sub>4</sub> emissions from lakes and reservoirs. *Sci. Rep.* **9**: 243. doi:[10.1038/s41598-018-36530-w](https://doi.org/10.1038/s41598-018-36530-w)
- Powell, R. J. 1972. Solubility of 16 gases in heptacosafuorotributylamine and carbon disulfide. *J. Chem. Eng. Data* **17**: 302–304. doi:[10.1021/jc60054a024](https://doi.org/10.1021/jc60054a024)
- R Core Team. 2016. R: A language and environment for statistical computing. R Foundation for Statistical Computing. Accessed on Dec 2016. Available from <https://www.R-project.org/>
- Repeta, D. J., S. Ferrón, O. A. Sosa, C. G. Johnson, L. D. Repeta, M. Acker, E. F. DeLong, and D. M. Karl. 2016. Marine methane paradox explained by bacterial degradation of dissolved organic matter. *Nat. Geosci.* **9**: 884–887. doi:[10.1038/ngeo2837](https://doi.org/10.1038/ngeo2837)
- RStudio Team. 2016. RStudio: Integrated development for R. RStudio, Inc. Available from <http://www.rstudio.com/>
- Saunio, M., and others. 2016. The global methane budget 2000–2012. *Earth Syst. Sci. Data* **8**: 697–751. doi:[10.5194/essd-8-697-2016](https://doi.org/10.5194/essd-8-697-2016)
- Signal Developers. 2013. signal: Signal processing. Accessed on June 2017. Available from <http://r-forge.r-project.org/projects/signal/>
- Tang, K. W., D. F. McGinnis, K. Frindte, V. Brüchert, and H.-P. Grossart. 2014. Paradox reconsidered: Methane oversaturation in well-oxygenated lake waters. *Limnol. Oceanogr.* **59**: 275–284. doi:[10.4319/lo.2014.59.1.0275](https://doi.org/10.4319/lo.2014.59.1.0275)
- Tang, W. K., D. F. McGinnis, D. Ionescu, and H.-P. Grossart. 2016. Methane production in oxic lake waters potentially increases aquatic methane flux to air. *Environ. Sci. Technol. Lett.* **3**: 227–233. doi:[10.1021/acs.estlett.6b00150](https://doi.org/10.1021/acs.estlett.6b00150)
- Thauer, R. K. 1998. Biochemistry of methanogenesis: A tribute to Marjory Stephenson: 1998 Marjory Stephenson Prize lecture. *Microbiology* **144**: 2377–2406. doi:[10.1099/00221287-144-9-2377](https://doi.org/10.1099/00221287-144-9-2377)
- Wang, Q., J. E. Dore, and T. R. McDermott. 2017. Methylphosphonate metabolism by *Pseudomonas* sp. populations contributes to the methane oversaturation paradox in an oxic freshwater lake. *Environ. Microbiol.* **19**: 2366–2378. doi:[10.1111/1462-2920.13747](https://doi.org/10.1111/1462-2920.13747)
- Whiticar, M. J. 1999. Carbon and hydrogen isotope systematics of bacterial formation and oxidation of methane. *Chem. Geol.* **161**: 291–314. doi:[10.1016/S0009-2541\(99\)00092-3](https://doi.org/10.1016/S0009-2541(99)00092-3)
- Yao, M., C. Henny, and J. A. Maresca. 2016. Freshwater bacteria release methane as a by-product of phosphorus acquisition. *Appl. Environ. Microbiol.* **82**: 6994–7003. doi:[10.1128/AEM.02399-16](https://doi.org/10.1128/AEM.02399-16)
- Zheng, Y., and others. 2018. A pathway for biological methane production using bacterial iron-only nitrogenase. *Nat. Microbiol.* **3**: 281–286. doi:[10.1038/s41564-017-0091-5](https://doi.org/10.1038/s41564-017-0091-5)

## Acknowledgments

Peter Casper at the Leibnitz Institute of Freshwater Ecology and Inland Fisheries (IGB) is acknowledged for giving access to a GC/FID unit and flux chamber. We thank Uta Mallok (IGB) for providing nutrient data. Further thanks to Elke Mach (IGB), Armin Penske (IGB), and Michael Sachtleben (IGB) for technical support. Anke Penzlin from the German Environment Agency (Umweltbundesamt) kindly provided weather data. Funding was provided by the German Research Foundation (GR1540/21-1, 23-1, 28-1), the German Ministry of Education and Science (BMBF 01LC1501G), and European Commission/Horizon program (H2020 project ERA-PLANET). Open access funding enabled and organized by Projekt DEAL.

## Conflict of Interest

None declared.

Submitted 30 May 2019

Revised 15 December 2019

Accepted 17 June 2020

Associate editor: Maria Maldonado